Chiba Medical J. 97E：1－10, 2021
doi:10.20776/S03035476-97E-1-P1

〔Chiba Medical Society Award Review〕

Advances in magnetic resonance neuroimaging of neuropathy from degenerative spinal disorders

Yawara Eguchi

Department of Orthopedic Surgery, Graduate School of Medicine, Chiba University, Chiba 260-8670.

（Received July 28, 2020, Accepted November 16, 2020, Published February 10, 2021.）

Abstract

It is challenging to use conventional magnetic resonance imaging（MRI）to diagnose external lesions of the spinal nerves, such as the brachial plexus, and lumbar nerves, which branch off the spinal cord. In addition, the use of MRI for the quantitative evaluation of nerve damage and chronic pain has been impossible. In recent years, neuroimaging techniques such as diffusion tensor imaging（DTI）have been developed with the increased magnetic field strength of clinical scanners and improvements in pulse sequences. Spinal nerve DTI is more prone to magnetic susceptibility than that in the brain, and has yet to reach widespread clinical application. However, reports indicate that information not available from conventional MRI can be obtained. The MR neurography/T2 mapping simultaneous imaging method, SHINKEI-Quant is based on T2 weighted imaging, has less distortion than DTI, and can be applied for the functional diagnosis of cervical nerve and brachial plexus injuries. Here, we discuss if visualization of spinal nerve lesions and the associated pain can be quantified by DTI and SHINKEI-Quant, and if further progress such as functional diagnosis of neuropathy may be possible.

Key words: **magnetic resonance imaging, MR neurography, diffusion tensor imaging, T2 mapping, lumbar foraminal stenosis, spinal nerves**

Ⅰ. Introduction

With the increasing age of our society, the number of patients with spinal disorders continues to rise. Pain signals are transmitted from local stimulation via the peripheral nerves and spinal cord to the brain, where they are perceived as pain. In recent years, functional magnetic resonance imaging（fMRI）[1]and MR spectroscopy[2]have commonly been employed as functional neuroimaging methods for the brain.

Lumbar nerve entrapment causes low back and leg pain, but discrepancies are often found between the clinical symptoms and the degree of nerve root compression on conventional MR images. For instance, disc abnormalities are frequently observed on images of asymptomatic patients[3,4]. Therefore, it can be difficult to understand physiologically the cause of the pain, and to provide a quantitative evaluation of

Address correspondence to Dr. Yawara Eguchi.
Department of Orthopaedic Surgery, Center for Orthopaedic Science Medical Innovation, Graduate School of Medicine, Chiba University, 1-8-1, Inohana, Chuou-ku, Chiba 260-8670, Japan.
Phone: +81-43-226-2117. Fax: +81-43-226-2116.
E-mail: yawara_eguchi@yahoo.co.jp

nerve damage. Another challenging issue is an imaging diagnosis of lumbar foraminal stenosis[5]. This is a condition in which nerve roots and lumbar nerves are entrapped in a narrowed lumbar foramen due to degenerative lumbar disorders. Macnab et al.[6] appropriately named lumbar foraminal stenosis the "hidden zone," as it is often overlooked. It accounts for approximately 60% of failed back surgery syndromes, and decreases surgical success rates[7] (Fig. 1A). Diagnostic imaging of lumbar spinal canal stenosis includes X-rays, CT, and MRI[8-10], along with functional diagnosis via selective nerve root imaging and infiltration[11]. Conventional MRI has a false positive rate of 30% to 40% in lumbar foraminal stenosis cases, which hampers diagnosis[12] (Fig. 1B). Using current MRI techniques it is challenging to diagnose external lesions of the spinal nerves, such as the brachial plexus, and lumbar nerves, which branch off the spinal cord, and a new imaging diagnostic method is needed.

In recent years, increased magnetic field strength of clinical scanners and improvement of pulse sequence have facilitated higher resolution neuroimaging. Various methods such as 3D MR neurography, diffusion-weighted MR neurography, and diffusion tensor imaging (DTI)[13-17]have been investigated for the non-invasive and selective visualization of peripheral nerves without use of contrast agents. Here, we discuss the latest findings to visualize radiculopathy due to the compressed spinal nerves using DTI and SHINKEI-Quant, which is a simultaneous imaging method for MR neurography/T2 mapping[18].

Ⅱ. DTI

Diffusion-weighted imaging (DWI) yields useful information regarding tissue microstructure because it monitors the random movement of water molecules, which is restricted by applying motion probing gradients (MPGs) in different directions[19-22]. DWI data can be used to determine quantitative values, such as the apparent diffusion coefficient (ADC). It is frequently used to diagnose central nervous system diseases, such as acute stroke[23], and is now widely used in clinical settings[24,25]. In addition, DWI can assess not only bulk diffusion, but also the direction of the diffusion of water molecules. In nerve fibers, the axonal cell membrane and myelin sheath restrict the diffusion in the direction cross-sectionally aligned to the nerve fiber bundle, which leads to a loss of water molecule isotropy. This condition is referred to as anisotropic diffusion, and both DTI and tractography are examples of selective analyses, which uses this information. Nerve damage can be quantitatively evaluated using the index of fractional anisotropy (FA), which indicates the strength

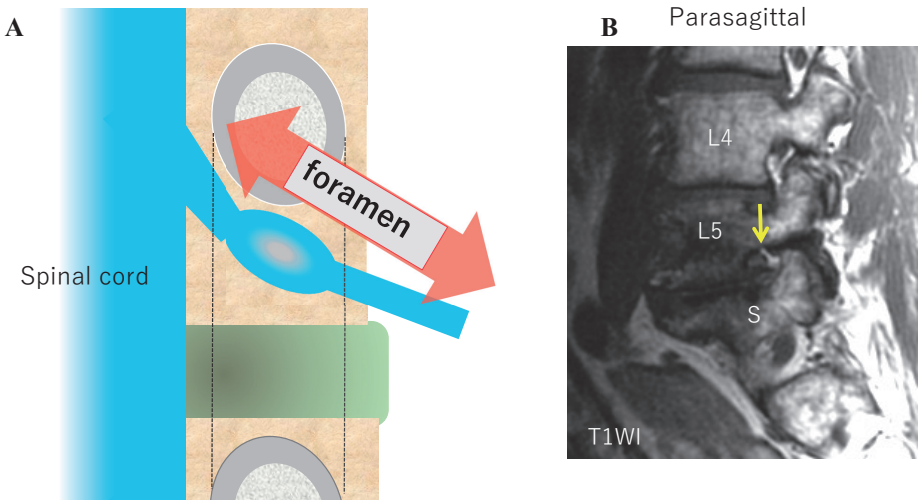

Fig. 1 Imaging of lumbar foraminal stenosis. (**A**) The spinal nerves branch outward from the spinal canal and extend through the foramina formed between the pedicles. Lumbar foraminal stenosis is a condition in which the nerve roots are constricted inside and outside the foramen. (**B**) On conventional MRI this condition is diagnosed by the disappearance of the fat signal in the parasagittal image. However, the false positive rate is as high as 40%[12]. From Eguchi et al., modified with permission[17].

of diffusion anisotropy. FA is a parameter of anisotropic strength and is expressed in values from 0 to 1. The closer the value is to 1, the stronger the anisotropy, while a value of 0 represents complete isotropy. Generally, when nerve damage occurs, the diffusion anisotropy along the nerve fibers decreases and the FA values also decrease[26,27]. In recent years, the usefulness of DTI for demyelinating and degenerative diseases such as multiple sclerosis, and peripheral nerve chronic compression lesions such as carpal tunnel syndrome has been reported[28,29]. Although the use of DTI in the spinal cord has been reported as well, the spine and spinal cord are more prone to magnetic susceptibility than the brain and thus it remains limited in clinical applications. DTI of the lumbar nerve roots has been investigated since 2011 and reports have increased rapidly in recent years[13-16] (Fig. 2A). It may be possible to quantitatively evaluate lumbar neuropathy by tractography findings and changes in DTI parameters such as ADC and FA values.

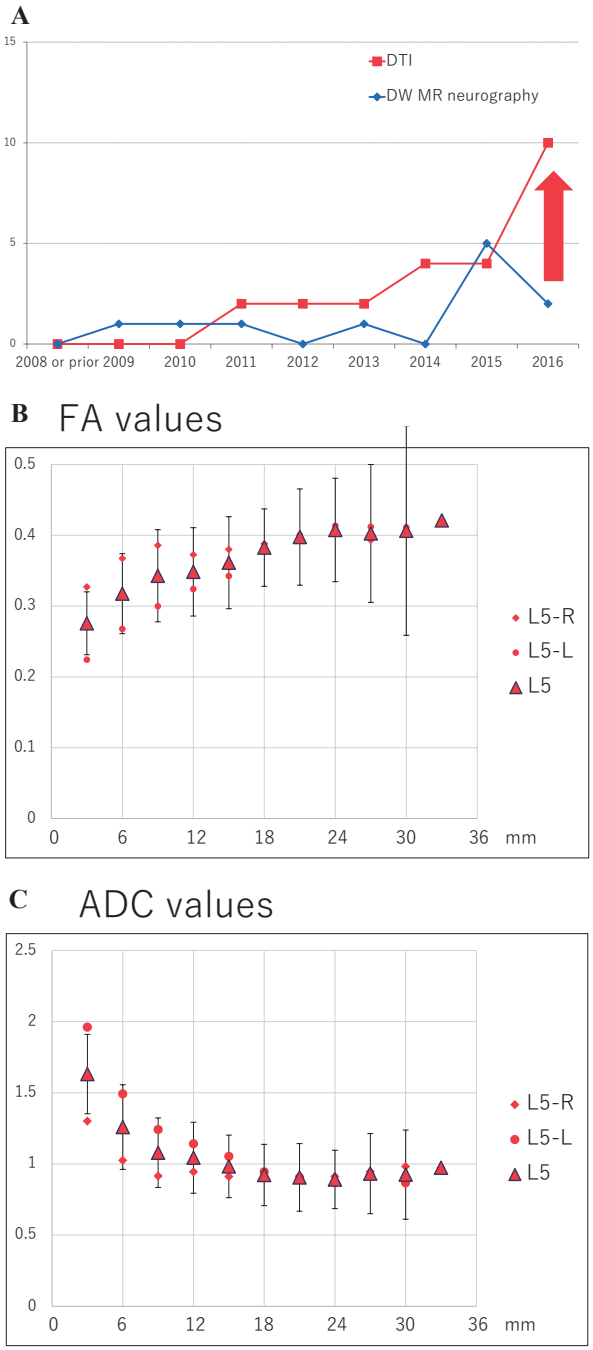

Fig. 2 The number of publications per year reporting DTI and DW neurography and FA values and ADC values of the DTI parameters. (**A**) The number of publications per year reporting DTI and DW neurography of the lumbar nerves. In recent years, DTI reports have increased rapidly. (**B**) FA values and (**C**) ADC values of the DTI parameters from the spinal bifurcation to distal of the L5 nerve roots in 40 healthy subjects. From Eguchi et al., modified with permission[17].

Ⅱ - a. Diagnosis of lumbar foraminal stenosis[13]

We measured the FA and ADC values from the spinal bifurcation to the distal part of the L5 nerves in 40 healthy volunteers (Fig. 2B, C). The FA values increased toward the distal part (Fig. 2B), and the ADC values were lower at the distal part (Fig. 2C). Then, we investigated the utility of DTI in the diagnosis of lumbar foraminal stenosis. A 3T MR imaging scanner (Discovery MR750; GE Healthcare, Milwaukee, WI, USA) was used. The DTI was performed with echo-planar imaging at a B value of 800 s/mm^2 and 11 directional MPGs. On the axial ADC and FA maps, regions of interest (ROIs) were placed in two locations, proximal and distal to the L3-S1 nerve root in the foramen, and the ADC and FA values of the lumbar nerve were measured. The lumbar nerve roots were visualized with tractography. In all subjects, the lumbar nerve roots were clearly visualized (Fig. 3A), and the tractography also showed abnormalities, such as tract disruption, nerve narrowing, and indentation of the course through the foramen (Fig. 3B). The FA value was significantly lower ($p < 0.001$, Fig. 3C) in the proximal and distal parts of the entrapped nerves than the intact nerves, and the ADC value was significantly increased ($p < 0.001$, Fig. 3D).

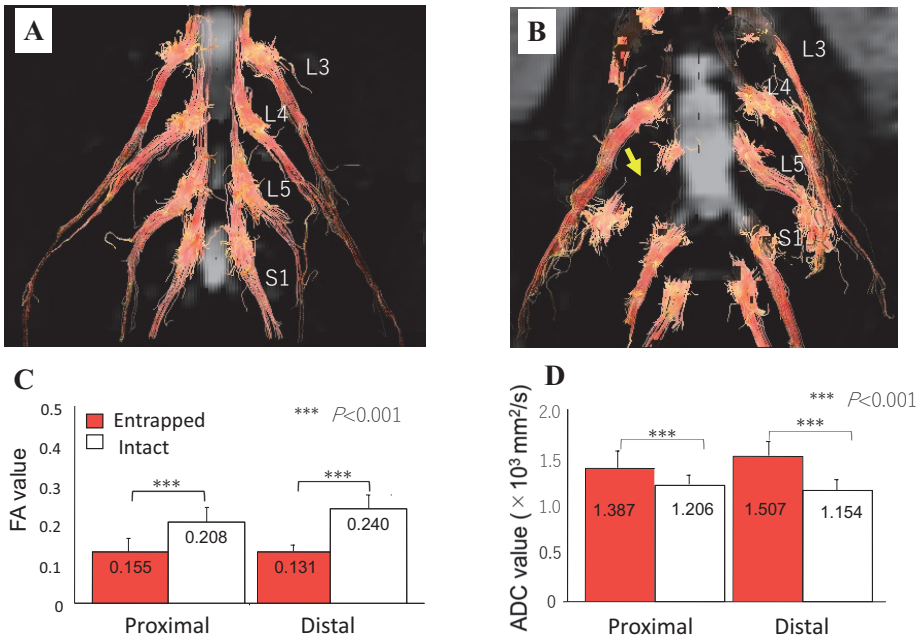

Fig. 3 Tractography of the lumbar nerves and DTI parameters. (**A**) Tractography of the lumbar nerves in healthy volunteers. L3, L3 nerve; L4, L4 nerve; L5, L5 nerve; S1, S1 nerve. (**B**) Tractography of the lumbar nerves of a patient with right L5 foraminal stenosis. The arrow indicates the tract of the right L5 nerve disruption in the foramen. (**C**) FA value and (**D**) ADC value result. The red bars indicate the entrapped side and white bars indicate the intact side. The FA values were significantly decreased ($p<0.001$) and the ADC values were significantly increased ($p<0.001$) in both the proximal and distal sides of the foramen, compared to the intact side. From Eguchi et al., modified with permission[17].

Ⅱ - b. Correlation between clinical symptoms and DTI parameters in patients with lumbar disc herniation[30]

Mixter and Barr[31]first described the radicular pain of sciatica as caused by spinal root compression of a herniated intervertebral disc. However, the underlying pathophysiology is not well understood. In clinical practice, asymptomatic intervertebral disc degeneration and herniation are found frequently, and the absence of pain in these cases can confuse spine surgeons[3,4]. We previously reported a correlation between neurological severity and DTI parameters, such as FA and ADC values, in patients with radiculopathy caused by lumbar disc herniation[33]. Microendoscopic surgery was performed in 11 cases with lumbar disc herniation. DTI was performed using a 1.5T MRI (Philips Medical Systems, Philips Electronics Japan, Achieva 1.5T Nova Dual) before and three months after surgery. The ROIs were defined in the distal parts of the nerve compression region (3-6 mm), and the average values of the FA and ADC were measured. For the severity of clinical symptoms, the Japanese Orthopedic Association (JOA; 0-29 points) scoring system, and the visual analogue scale (VAS) score for low back pain, leg pain, and leg numbness from 100 (extreme amount of pain) to 0 (no pain) were measured preoperatively and three months postoperatively. The tractography of the lumbar nerves in a 46-year-old man with lumbar disc herniation between L5 and S1 before and after microendoscopic discectomy (MED) indicated improved clinical symptoms (Fig. 4). The JOA score increased from 17 points preoperatively to 29 points posteoperatively. The tractography of the S1 nerve on the right side was disrupted with disc herniation before MED (Fig. 4A). Six months after MED, the FA value increased from 0.299 to 0.327, and the tractography of the S1 nerve elongated to the proximal side, . This correlated with neurologic improvement and the therapeutic effect (Fig. 4B). The FA value decreased and ADC increased in the damaged nerve. The preoperative JOA scores of injury severity and FA values correlated positively ($p<0.001$) and ADC values correlated negatively with JOA scores ($p<0.05$) (Fig. 4C, D). These findings indicate that the FA and ADC values obtained from diffusion tensor

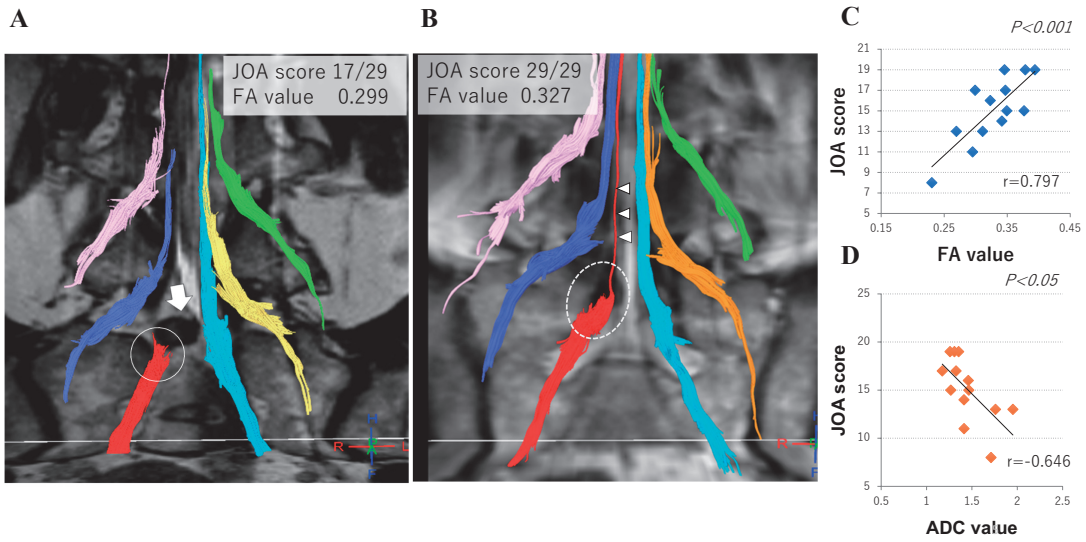

Fig. 4 Tractography before and after microendoscopic surgery for disc herniation and correlation between DTI parameters and symptoms. (**A**, **B**) Tractography before and after microendoscopic surgery for L5/S1 disc herniation. A: Before surgery, a right S1 nerve disruption is observed due to herniation (arrow). B: After surgery, the cauda equina is clearly visualized (arrowhead). The FA level increased as the symptoms improved. Regarding the FA and ADC values and the clinical symptoms JOA score. (**C**) The preoperative JOA scores and FA values were positively correlated ($r = 0.797$, $p < 0.001$). (**D**) The ADC values were negatively correlated ($r = -0.646$, $p < 0.05$). From Eguchi et al., modified with permission[17].

analysis correlate with the severity of clinical symptoms. DTI parameters may serve as an index of severity, which is required for a functional diagnosis of neuropathy.

Ⅱ - c. High resolution DTI

With the advent of 3T MRI, it became possible to rapidly obtain high-resolution images. However, due to the higher magnetic field strength, susceptibility effects and motion artifacts may cause signal irregularities and image distortions. There are limitations to the nerve fiber tracking in regions that are prone to artifacts, and further improvement in image resolution is essential for future clinical applications.

A new reduced field-of-view FOV (rFOV) single-shot, diffusion-weighted, echo-planar imaging method has been proposed. This approach uses a 2D spatially selective echo-planar radio frequency excitation pulse and a 180° refocusing pulse to reduce the FOV in the phase-encode (PE) direction, and simultaneously suppresses the signal from fat. The rFOV method decreases the readout duration and allows the acquisition of high-resolution diffusion-weighted images for practical applications to spinal imaging[32]. We attempted high-resolution imaging of the lumbar nerves with rFOV 3T MRI. Compared to traditional methods, rFOV provides clear visualization of the lumbar nerves and enables accurate quantification of the FA and ADC values[33] (Fig. 5A). Furthermore, by applying multi-band SENSE and increasing the number of MPG axes to 128, we succeeded in obtaining clear tractography [34] (Fig. 5B). In the future, these high-resolution DTI methods may be used to visualize nerve injuries and improve the accuracy of DTI parameter quantification with increased opportunities for clinical applications.

Ⅲ. Functional diagnosis of cervical radiculopathy using SHINKEI-Quant [18]

It is difficult to visualize cervical nerves by DTI because the neck region is distorted by surrounding motion artifacts from the lung and there is a high degree of magnetic susceptibility anisotropy. There is no diagnostic imaging method to quantitatively evaluate cervical radiculopathy. The three-dimensional nerve-sheath signal is increased with inked rest-tissue rapid acquisition of relaxation imaging (SHINKEI)[35], a type of new MR neurography technique that suppresses

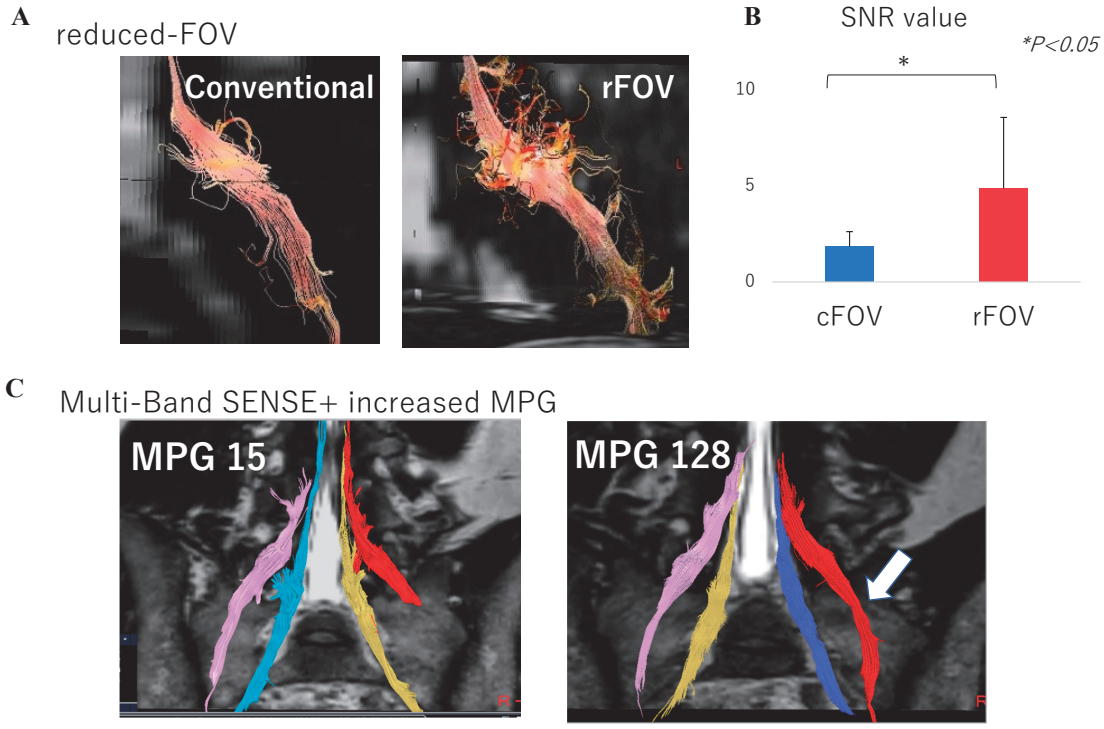

Fig. 5 High resolution DTI. (**A**, **B**) The reduced FOV SNR was improved by the reduced FOV method. (**C**) With multi-band SENSE and increasing the number of MPGs axes to 128, a clearer tract of the lumbar nerves was obtained. In the spinal canal, SNR values were 4.87 ± 3.70 for rFOV and 1.84 ± 0.78 for cFOV, showing a significantly high SNR with rFOV compared with cFOV. In MPG128 axis, the lumbar nerve is clearly drawn to the distal side compared with 15 axis (arrow). From Eguchi et al., modified with permission [17].

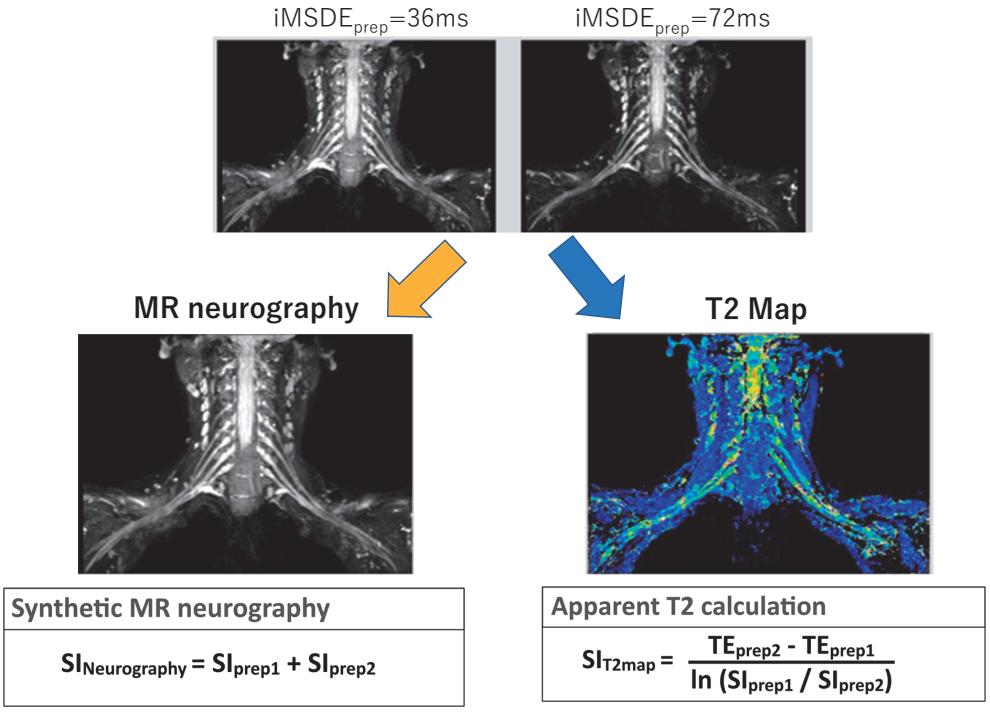

Fig. 6 SHINKEI-Quant. MR Neurography is a method used to evaluate nerve morphology by imaging only the nerves by blood flow signal suppression pulses called iMSDE from T2-weighted images obtained with Turbo spin-echo. SHINKEI Quant can acquire a T2 map automatically and simultaneously from MR neurography taken at two different echo times (36ms, 72ms), and can quantitatively evaluate nerve lesions based on T2 values simultaneously with the morphological evaluation. From Yoneyama et al., modified with permission [35].

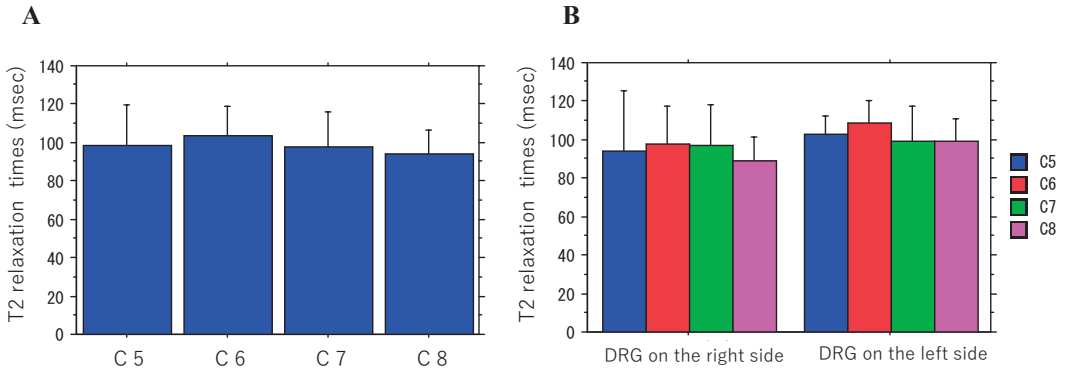

Fig. 7 Cervical nerve DRG T2 relaxation times in healthy individuals. (**A**) T2 relaxation times (ms) at each spinal level. The T2 relaxation times (ms) at each spinal level were 98.7 ± 21.0, 103.2 ± 15.7, 98.1 ± 17.6, and 93.9 ± 12.3 for C5, C6, C7, and C8 nerve roots, respectively. We observed no significant differences in the nerve root T2 values at each spinal level ($p < 0.05$). (**B**) The T2 relaxation times (ms) for bilateral nerve roots at each spinal level (right side, left side, p value). We also observed no significant differences between the left- and right-sided nerve roots: C5 nerve root 94.4 ± 31.1, 103.1 ± 8.9, $p = 0.67$, C6 nerve root 97.7 ± 20.0, 108.7 ± 11.3, $p = 0.19$, C7 nerve root 96.7 ± 21.2, 99.4 ± 17.8, $p = 0.68$, C8 nerve root 88.9 ± 12.8, 99.1 ± 11.8, $p = 0.085$. From Eguchi et al., modified with permission[18].

the signal from blood vessels, muscles, and fat using improved motion-sensitive driven equilibrium (iMSDE) and spectral attenuated inversion recovery. SHINKEI allows the morphological evaluation of the cervical nerve roots. However, the technique lacks the capacity to quantify the status of the nerve roots. Recently, Yoneyama et al. reported the development of SHINKEI-Quant, an advanced sequence that can acquire MR neurography and simultaneously allow quantitative evaluation of T2 relaxation times (Fig. 6). Five healthy male subjects with a mean age of 37 years underwent simultaneous apparent T2 mapping and neurography with SHINKEI-Quant using a 3T MRI (manufactured by Philips, Ingenia CX). In the healthy subjects, there was no significant difference in the T2 relaxation times between spinal levels (Fig. 7A) or between the left and right nerve roots at each spinal level (Fig. 7B)[18].

Case presentation

A 49-year-old man developed pain radiating from the area around the right scapula to the right forearm and numbness of the fingers in his right hand two months before consulting us (Fig. 8)[18]. T2 weighted magnetic resonance imaging (MRI) showed right-sided herniation of the C6-7 intervertebral disc. We also observed right-sided herniation of the intervertebral disc at the level of C4-5, which confounded the diagnosis (Fig. 8A-C). Neurography revealed swelling of the right C7 nerve in our patient (Fig. 8D). There was no significant difference in T2 relaxation times between the C5 nerve roots on the left- and right sides (left: 89, right: 82), but the T2 relaxation time was significantly prolonged in the right C7 nerve root (left: 127, right: 74; Fig. 8E, F).

Based on these findings, we diagnosed the patient with C7 radiculopathy due to C6-7 intervertebral disc herniation. We performed decompression of the C7 nerve by microendoscopic surgery in this patient (Fig. 8G, H).

The patient was able to return to work one month after surgery, and the right upper arm pain had improved dramatically six months after surgery.

Ⅳ. Comparison of DTI and SHINKEI-Quant

The mean imaging time for DTI is 4 min and 54 s, compared to 7 min and 12 s for the SHINKEI-Quant technique. However, during DTI, the nerve is outlined manually as the ROI to create the tractogram, whereas the SHINKEI-Quant technique allows neurography to be acquired automatically. DTI is affected by distortion, whereas visualization by neurography is unaffected by distortion, a major advantage. The use of DTI for lumbar nerve lesions can, with high accuracy, reveal significant

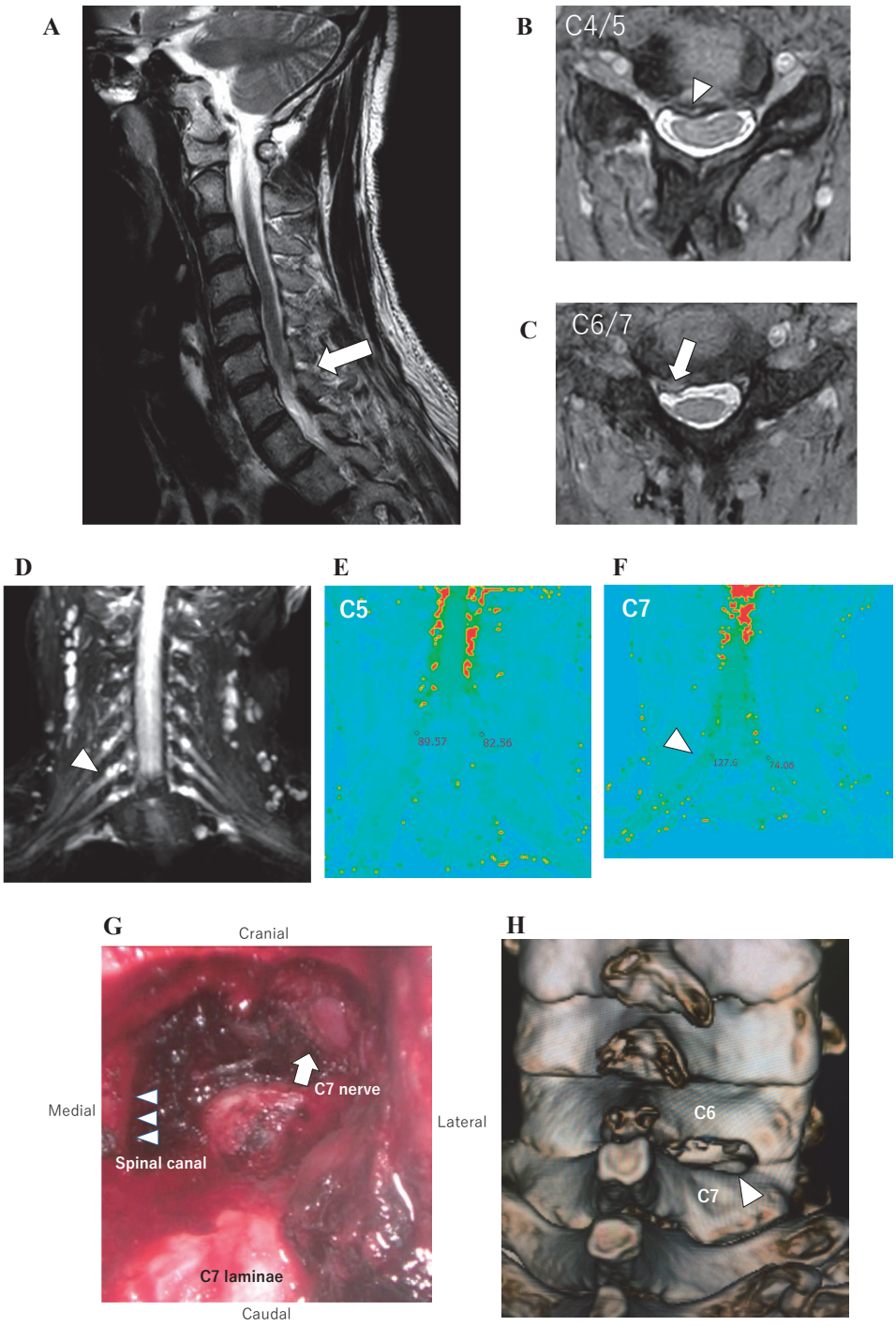

Fig. 8 Imaging and surgical findings of an example case. (**A**) Preoperative MRI sagittal image (T2-weighted image) of the cervical spine. Herniation of the C6-7 intervertebral disc can be observed (arrow). (**B**) Preoperative axial MRI image of C4-5. Right-sided intervertebral disc herniation with mild spinal cord compression (arrowhead) was observed. (**C**) Preoperative axial MRI image of C6-7. Right-sided intervertebral disc herniation (arrowhead) was observed. (**D**) Cervical neurography (coronal image). Swelling of the right C7 nerve (arrowhead). (**E**) Cervical T2 mapping (coronal image) of C5 nerve There was no significant difference in T2 relaxation times (ms) between the C5 nerve roots on the left- and right sides (left: 89, right: 82). (**F**) Cervical T2 mapping of C7 nerve. The T2 relaxation time was significantly prolonged in the right C7 nerve root (left: 127, right: 74) (arrowhead). (**G**) Intraoperative photograph during microendoscopic surgery. We resected the inferior margin of the C6 lamina, and the superior margin of the C7 lamina, then removed the medial C6-7 facet joint, and exposed the area from the lateral margin of the dura mater (arrowhead) to the C7 nerve bifurcation (arrow). (**H**) Postoperative 3D-CT image of the cervical spine. The fenestration of the inferior margin of the C6 lamina, the superior margin of the C7 lamina, and the medial third of the C6-7 facet joint (arrowhead) were confirmed. From Eguchi et al., modified with permission[18].

decreases in fractional anisotropy（FA）and significant increases in the apparent diffusion coefficient（ADC）for compression lesions[30]. There are few reports that include the T2 relaxation times in patients with nerve injuries, and in the future, we will obtain additional evidence by accumulating more cases.

Ⅴ. Conclusion

In recent years, neuroimaging techniques, such as DTI, have been developed that take advantage of the increasing magnetic field strength of clinical scanners and improvements in pulse sequences. Spinal nerve DTI is more prone to magnetic susceptibility than the brain, and has yet to reach widespread clinical application. However, information not available from conventional MRI can be obtained. The MR neurography/T2 mapping simultaneous imaging method, SHINKEI-Quant is based on T2 weighted imaging and has less distortion than DTI. It can be applied to the functional diagnosis of cervical nerve and brachial plexus injuries. Visualization of spinal nerve lesions and the associated pain can be quantified numerically by DTI and SHI1NKEI-Quant, and in the future a functional diagnosis of neuropathy may be possible.

Financial support

This study was supported in part by Mitsui Sumitomo Insurance Welfare Foundation, the Nakatomi Foundation, ZENKYOREN（National Mutual Insurance Federation of Agricultural Cooperatives）.

Conflict of interest

The author declares no competing interests.

Ethical approval

Not applicable.

Data availability

Not applicable.

Acknowledgment

I thank Professor Seiji Ohtori for critically reading this manuscript.

References

1）Kobayashi Y, Kurata J, Sekiguchi M, Kokubun M, Akaishizawa T, Chiba Y, Konno S, Kikuchi S.（2009）Augmented cerebral activation by lumbar mechanical stimulus in chronic low back pain patients: an FMRI study. Spine 34, 2431-6.
2）Shigemura T, Kishida S, Eguchi Y, Ohtori S, Nakamura J, Kojima M, Masuda Y, Takahashi K.（2012）Proton magnetic resonance spectroscopy of the thalamus in patients with osteoarthritis of the Hip. Bone Joint Res 1, 8-12.
3）Boden SD, Davis DO, Dina TS, Patronas NJ, Wiesel SW.（1990）Abnormal magnetic-resonance scans of the lumbar spine in asymptomatic subjects. A prospective investigation. J Bone Joint Surg Am 72, 403-8.
4）Jensen MC, Brant-Zawadzki MN, Obuchowski N, Modic MT, Malkasian D, Ross JS.（1994）Magnetic resonance imaging of the lumbar spine in people without back pain. N Engl J Med 331, 69-73.
5）Jenis LG, An HS.（2000）Spine update. Lumbar foraminal stenosis. Spine 25, 389-94.
6）MacNab I.（1971）Negative disc exploration: an analysis of the causes of nerve root involvement in sixty-eight patients. J Bone Joint Surg Am 53, 891-903.
7）Burton R, Kirkaldy-Willis W, Yong-Hing K, Heithoff K.（1981）Causes of failure of surgery on the lumbar spine. Clin Orthop 157, 191-7.
8）Hasegawa T, An H, Haughton V, Nowicki B.（1995）Lumbar foraminal stenosis: critical heights of the intervertebral discs and foramina. J Bone Joint Surg 77, 32-38.
9）Kirkaldy-Willis W, Wedge J, Yong-Hing K, Tchang S, de Kjorompay V, Shannon R.（1982）Lumbar spinal nerve lateral entrapment. Clin Orthop 169, 171-8.
10）Vanderlinden RG.（1984）Subarticular entrapment of the dorsal root ganglion as a cause of sciatic pain. Spine 9, 19-22.
11）Herron L.（1989）Selective nerve root block in patient selection for lumbar surgery:surgical results. J Spinal Disord 2, 75-79.
12）Aota Y, Niwa T, Yoshikawa K, Fujiwara A, Asada T, Saito T.（2007）Magnetic resonance imaging and magnetic resonance myelography in the presurgical diagnosis of lumbar foraminal stenosis. Spine 32, 896-03.

13) Eguchi Y, Ohtori S, Orita S, Kamoda H, Arai G, Ishikawa T, Miyagi M, Inoue G, Suzuki M, Masuda Y, Andou H, Takaso M, Aoki Y, Toyone T, Watanabe A, Takahashi K. (2011) Quantitative evaluation and visualization of lumbar foraminal nerve root entrapment using diffusion tensor imaging: preliminary results. Am J Neuroradiol 32, 1824-9.
14) Balbi V, Budzik JF, Duhamel A, Bera-Louville A, Le Thuc V, Cotten A. (2011) Tractography of lumbar nerve roots: initial results. Eur Radiol 21, 1153-9.
15) van der Jagt PK, Dik P, Froeling M, Kwee TC, Nievelstein RA, ten Haken B, Leemans A. (2012) Architectural configuration and microstructural properties of the sacral plexus: a diffusion tensor MRI and fiber tractography study. Neuroimage 62, 1792-9.
16) Budzik JF, Verclytte S, Lefebvre G, Monnet A, Forzy G, Cotten A. (2013) Assessment of reduced field of view in diffusion tensor imaging of the lumbar nerve roots at 3 T. Eur Radiol 23, 1361-6.
17) Eguchi Y, Kanamoto H, Oikawa Y, Suzuki M, Yamanaka H, Tanai H, Kobayashi T, Orita S, Yamauchi K, Suzuki M, Inage K, Aoki Y, Watanabe A, Furuya T, Koda M, Takahashi K, Ohtori S. (2017) Recent advances in magnetic resonance neuroimaging of lumbar nerve to clinical applications: a review of clinical studies utilizing diffusion Tensor Imaging and Diffusion-weighted MR neurography. Spine Surg Relat Res 1, 61-71.
18) Eguchi Y, Enomoto K, Sato T, Watanabe A, Sakai T, Norimoto M, Yoneyama M, Aoki Y, Suzuki M, Yamanaka H, Tamai H, Kobayashi T, Orita S, Suzuki M, Inage K, Shiga Y, Hirosawa N, Inoue M, Koda M, Furuya T, Nakamura J, Hagiwara S, Akazawa T, Takahashi H, Takahashi K, Ohtori S. (2020) Simultaneous MR neurography and apparent T2 mapping of cervical nerve roots before microendoscopic surgery to treat patient with radiculopathy due to cervical disc herniation: preliminary results. J Clin Neurosci 74, 213-19.
19) Basser PJ, Jones DK. (2002) Diffusion tensor MRI: theory, experimental design and data analysis-a technical review. NMR Biomed 15, 456-67.
20) Beaulieu C, Allen PS. (1994) Determinants of anisotropic water diffusion in nerves. Magn Reson Med 31, 394-400.
21) Beaulieu C, Does MD, Snyder RE, Allen PS. (1996) Changes in water diffusion due to Wallerian degeneration in peripheral nerve. Magn Reson Med 36, 627-31.
22) Basser PJ, Pierpaoli C. (1996) Microstructural and physiological features of tissues elucidated by quantitative-diffusion-tensor MRI. J Magn Reson B 111, 209-19.
23) Minematsu K, Fisher M, Li L, Davis MA, Knapp AG, Cotter RE, McBurney RN, Sotak CH. (1992) Diffusion-weighted magnetic resonance imaging: rapid and quantitative detection of focal brain ischemia. Neurology 42, 235-40.
24) Lin X, Tench CR, Morgan PS, Constantinescu CS. (2008) Use of combined conventional and quantitative MRI to quantify pathology related to cognitive impairment in multiple sclerosis. J Neurol Neurosurg Psychiatry 79, 437-44.
25) Mamata H, Jolesz FA, Maier SE. (2005) Apparent diffusion coefficient and fractional anisotropy in spinal cord: age and cervical spondylosis-related changes. J Magn Reson Imaging 22, 38-43.
26) Takagi T, Nakamura M, Yamada M, Hikishima K, Momoshima S, Fujiyoshi K, Shibata S, Okano HJ, Toyama Y, Okano H. (2009) Visualization of peripheral nerve degeneration and regeneration: monitoring with diffusion tensor tractography. Neuroimage 44, 884-92.
27) MacDonald CL, Dikranian K, Bayly, P, Holtzman D, Brody D. (2007) Diffusion tensor imaging reliably detects experimental traumatic axonal injury and indicates approximate time of injury. J Neurosci 27, 11869-76.
28) Khalil C, Hancart C, Le Thuc V, Chantelot C, Chechin D, Cotton A. (2008) Diffusion tensor imaging and tractography of the median nerve in carpal tunnel syndrome: preliminary results. Eur Radiol 18, 2283-91.
29) Lehmann HC, Zhang J, Mori S, Sheikh KA. (2010) Diffusion tensor imaging to assess axonal regeneration in peripheral nerves. Exp Neurol 223, 238-44.
30) Eguchi Y, Oikawa Y, Suzuki M, Yamanaka H, Tamai H, Kobayashi T, Orita S, Yamauchi K, Suzuki M, Aoki Y, Watanabe A, Takahashi K, Ohtori S. (2016) Diffusion tensor imaging parameters of radiculopathy in patients with lumbar disc herniation: preliminary results. The Bone Joint J 98-B, 387-94.
31) Mixter WJ, Barr JS. (1934) Rupture of the intervertebral disc with involvement of the spinal canal. N Engl J Med 211, 210-5.
32) Saritas EU, Cunningham CH, Lee JH, Han ET, Nishimura DG. (2008) DWI of the spinal cord with reduced FOV single-shot EPI. Magn Reson Med 60, 468-73.
33) Kanamoto H, Eguchi Y, Oikawa Y, Orita S, Inage K, Fujimoto K, Shiga Y, Abe K, Inoue M, Kinoshita H, Matsumoto K, Masuda Y, Furuya T, Koda M, Aoki Y, Watanabe A, Takahashi K, Ohtori S. (2017) Visualization of lumbar nerves using reduced field of view diffusion tensor imaging in healthy volunteers and patients with degenerative lumbar disorders. Br J Radiol 90: 20160929.
34) Norimoto M, Eguchi Y, Watanabe A, Sakai T, Murayama D, Yoneyama M, Kawasaki Y, Furuya T, Orita S, Inage K, Shiga Y, Maki S, Inoue M, Umimura T, Sato T, Sato M, Suzuki M, Enomoto K, Aoki Y, Ohtori S. (2020) Does the increased motion probing gradient directional diffusion tensor imaging of lumbar nerves using Multi-Band SENSE improve the visualization and accuracy of FA values? Eur Spine J 29, 1693-701.
35) Yoneyama M, Togao O, Hiwatashi A, Ozawa Y, Obara M, Okuaki T, Cauteren MV. (2016) SHINKEI quant: simultaneous acquisition of MR neurography and T2 mapping for quantitative evaluation of chronic inflammatory demyelinating polyneuropathy. Proc Int Soc Magn Reson Med 24, 1322.